# Polarized Cu *K* edge XANES spectra of CuO – theory and experiment

**Ondřej Šipr,**[a]* **Antonín Šimůnek,**[a]
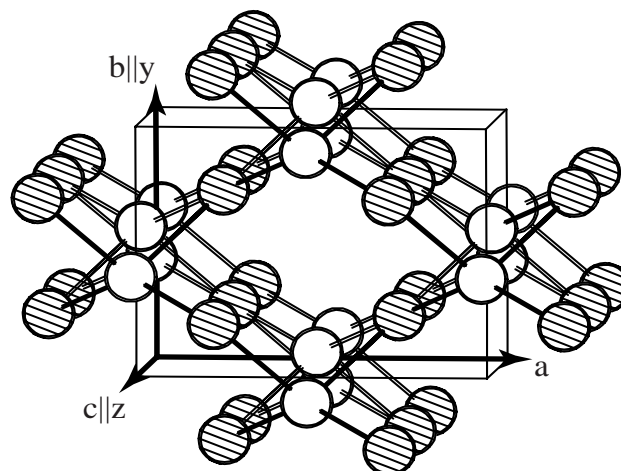**Sergey Bocharov,**[b] **Thomas Kirchner**[b] **and**
**Günther Dräger**[b]

*[a]Institute of Physics, Academy of Sciences of the Czech Republic, Cukrovarnická 10, 162 53 Prague, Czech Republic, and [b]Martin-Luther-Universität Halle-Wittenberg, Friedemann-Bach-Platz 6, D-06108 Halle, Germany. E-mail: sipr@fzu.cz*

**Figure 1**
CuO structure in the the cell reference frame *xyz*. Hatched circles are copper atoms, white circles are oxygens. The *y* and *z* axes are fixed by crystallographic axes ($y\|b, z\|c$) while *x* is orthogonal to them, being thus rougly colinear with *a*.

Polarized Cu *K* edge x-ray absorption near-edge structure (XANES) spectra of CuO are analyzed. Partial spectral components reflecting both dipole and quadrupole transitions are resolved from the experiment. Theoretical spectra were obtained using the real-space multiple-scattering technique and by calculating the band structure via the pseudopotential method. We demonstrate that the pre-peak is of a quadrupole character and find its decomposition into individual *d* components. The self consistent pseudopotential calculation, free from any constraints on the form of the potential, improves the agreement between theory and experiment in those areas where real-space calculation, based on non-self-consistent muffin-tin potential, fails. Therefore we argue that the most significant contributions to the Cu *K* edge XANES come from one-electron processes.

**Figure 2**
Local reference frame $x'y'z'$ defined by the central copper atom and the nearest four oxygens. The $x'$ axis is parallel to longer side of the $O_4$ parallelogram, the $y'$ axis lies within the $CuO_4$ plane perpendicularly to $x'$, and $z'$ is perpendicular both to $x'$ and $y'$. All lengths in the scheme are in angströms.

## 1. Introduction

Copper oxide CuO serves as a model compound for interpreting x-ray absorption near-edge structure (XANES) spectral features in more complex materials, such as high-$T_c$ superconductors. In particular, this applies to the Cu *K* edge spectrum as well. However, common understanding of dominant spectral features and, especially, of the pre-peak in the Cu *K* edge XANES of CuO mostly arises from indirect evidence. Typically, experimental and theoretical investigation concentrated rather on related compounds containing $CuCl_2$ or $CuCl_4^{-2}$ molecular complexes (Bair and Goddard, 1980; Yokoyjama *et al.*, 1986; Hahn *et al.*, 1982). Investigations of proper CuO were limited to unpolarized spectra only (Normal *et al.*, 1985; Šipr, 1992), severely thus restricting their relevance for clarification of origin of spectral features in other compounds.

Only recently Bocharov *et al.* (2001) undertook a comprehensive study of *polarized* Cu *K* edge spectra of CuO, comparing partial spectral components resolved from experimental data with results of a real-space multiple-scattering (RS-MS) calculation for a non-self consistent muffin-tin potential. Although a general agreement between theoretical and experimental spectra has been observed, perceptible inaccuracies of the theory at certain energy ranges and/or polarizations have been recognized. Such failures could indicate either insufficiency of the non-self consistent muffin-tin potential employed in the calculation or, alternatively, may point to the inability of the one-electron local density approximation (LDA) formalism itself to describe certain spectral transitions. Indeed, many-body origin of the shoulder structure in Cu *K* edge XANES of CuO was suggested by Bair & Goddard (1980) or Yokoyama *et al.* (1986).
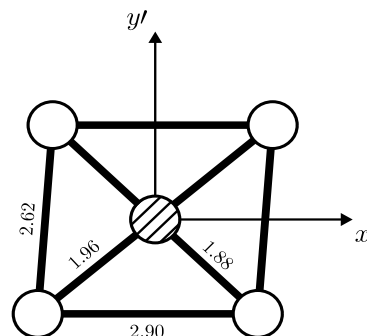
In order to cast more light on this issue, we compare the experimental and RS-MS results with yet another set of theoretical curves obtained from a *self consistent* band-structure calculation based on the pseudopotential technique, *by-passing thus the muffin-tin constraint*.

## 2. Spectral decomposition

Any linearly polarized XANES spectrum $\mu$ can be decomposed into a weighted sum of few dipole $\mu_i^{(\mathrm{dip})}$ and quadrupole $\mu_j^{(\mathrm{qdr})}$ partial spectral components,

$$\mu = \sum_i c_i^{(\mathrm{dip})} \mu_i^{(\mathrm{dip})} + \sum_j c_j^{(\mathrm{qdr})} \mu_j^{(\mathrm{qdr})} , \qquad (1)$$

where the partial spectral weights $c_i^{(\mathrm{dip})}$ and $c_j^{(\mathrm{qdr})}$ are determined by the orientation of the polarization vector $\varepsilon$ and wave vector $\boldsymbol{k}$ of the exciting x-ray radiation with respect to the sample.

For the *K* edge, final states have either *p* or *d* symmetry for the dipole or quadrupole transitions, respectively. The monoclinic crystal structure of CuO induces four dipole $\mu_i^{(\mathrm{dip})}$ and nine quadrupole $\mu_j^{(\mathrm{qdr})}$ partial spectral components in total (Brouder,

1990). However, in order to stay with physically transparent concepts and to facilitate comparison with earlier works, we restrict ourselves just to three dipole and five quadrupole components, which have their counterparts among partial $\ell, m$-projected densities of states. We present an extensive discussion and arguments in favour of fairness of this restriction in Bocharov *et al.* (2001). Here we only note that if the reduction of the number of partial components were unjustified, it would not be have been possible to decompose the experimental spectra along Eq. (1) in a unique way. Such a decomposition, nevertheless, cannot be made in an arbitrary coordinate system. We identified two suitable frames for CuO: One that is attached to the crystal unit cell (Fig. 1), and another — a local one — adjusted to the nearest neighborhood of a Cu atom (Fig. 2).

## 3. Experimental and theoretical methods

The spectra were measured in a transmission mode at the beam lines A1 and E4 (HASYLAB, DESY), using a Si (111) two crystal monochromator. The sample plate was positioned in a PC-controlled goniometer allowing three perpendicular rotations, so that any orientation of the sample with respect to the polarization vector $\varepsilon$ and the wave vector $\boldsymbol{k}$ can be adjusted. As described in Bocharov *et al.* (2001) in detail, experiment-based partial spectral components in both cell and local coordinate systems were extracted from several sets of measured "raw" polarized spectra via inversion of Eq. (1).

The RS-MS theoretical curves were calculated for a cluster of 135 atoms. Non-self-consistent muffin-tin potentials were generated via the so-called Mattheiss prescription. The influence of the core hole left by the excited electron was taken into account by moving a 1$s$ electron from the core into the lowest unoccupied atomic level. Individual partial spectral components were evaluated by calculating XANES spectra for suitably chosen orientation of the $\varepsilon$ and $\boldsymbol{k}$ vectors.

The electronic structure of CuO was calculated self-consistently by a pseudopotential method within the LDA. We have used a plane-wave basis that imposes no shape approximations on either the charge density or the potential. We employed pseudopotentials generated not from the ground state electron configuration of free atoms but rather from the crystal charge density, using the iterative technique of Vackář *et al.* (1998).

The technical details of the calculations of x-ray spectra in the pseudopotential formalism were described in detail by Šimůnek *et al.* (1995). Here we note that the radial parts of the dipole and quadrupole matrix elements were approximated by constants, and only their angular parts use the plane-wave basis set mentioned above.

All theoretical results presented here include the convolution with a Lorentzian function of full width at half-maximum of 1.5 eV, accounting thus for the 1$s$ core hole lifetime.

## 4. Results and discussion

The symmetry-resolved dipole partial spectral components in the cell and in the local reference frames are shown in Fig. 3 and Fig. 4, respectively. The quadrupole components are displayed in Fig. 5 for both frames. The origin of the energy scale coincides with the Fermi level provided by the band-structure calculation, the horizontal alignment between different sets of curves was chosen so that the best overall agreement between peak positions is achieved. The zero energy corresponds thus to the 8980 eV energy of the exciting radiation for the experimental curves. The vertical

scales for all the three families of curves were again fitted for the best overall agreement. As indicated in Fig. 5, the quadrupole components were multiplied by ten (experimental curves) and by five (real-space curves) to make their details more visible. The height of band-structure quadrupole components is arbitrary.
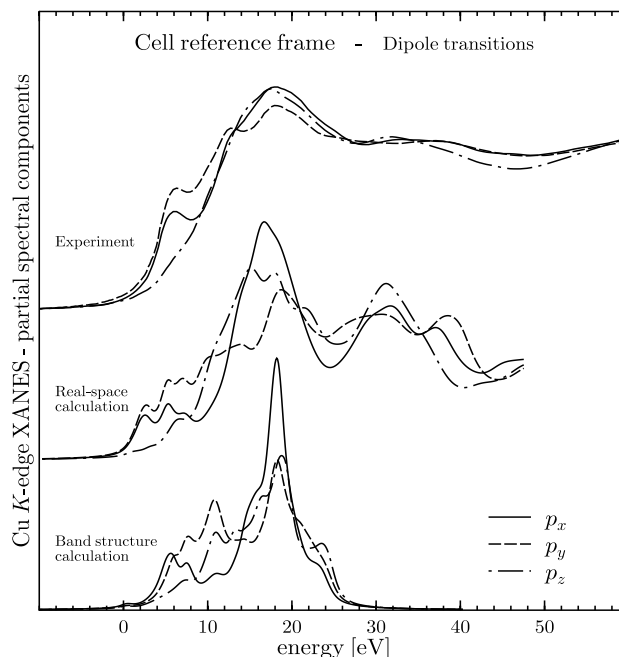


**Figure 3**
Dipole components of polarized Cu $K$ edge XANES of CuO in a cell reference frame, obtained by analyzing the experimental data and via RS-MS and band-structure calculation.
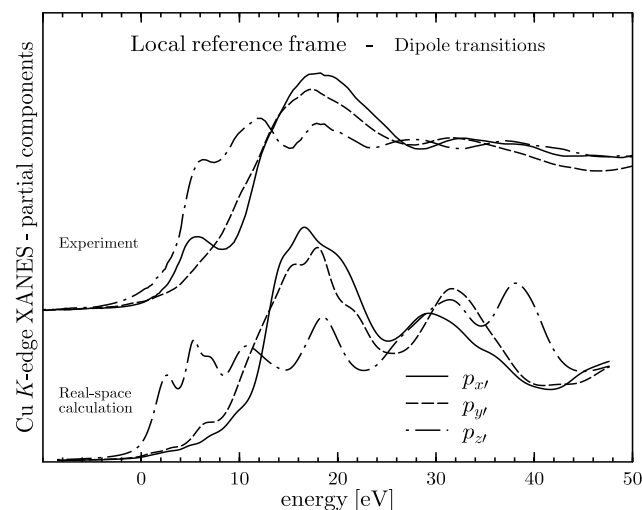


**Figure 4**
Dipole components of polarized Cu $K$ edge XANES of CuO in a local reference frame, obtained by analyzing the experimental data and via a RS-MS calculation.
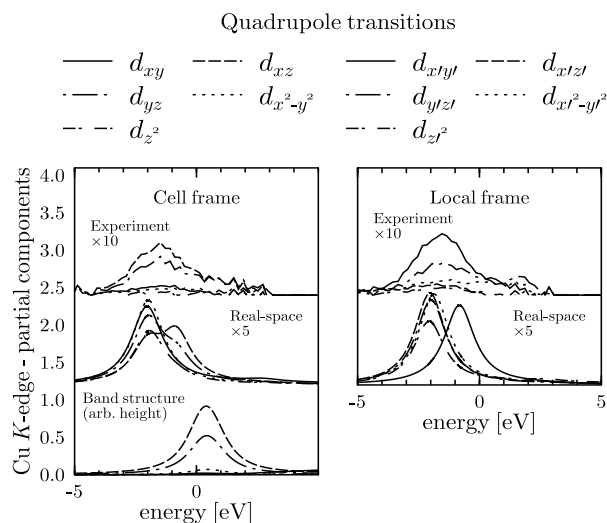
**Figure 5**
Quadrupole components of polarized Cu $K$ edge XANES of CuO in both the cell and the local reference frames, obtained by analyzing the experimental data and via RS-MS and band-structure calculation. In order to make the details more visible, the height of experimental peaks was multiplied by ten and the height of RS-MS theroetical peaks was multiplied by five with respect to the vertical scale of Figs. 3–4. The height of the band-structure quadrupole is arbitrary.

The band-structure calculation was performed only in the cell coordinate system (Fig. 2), including all bands up to 25 eV above the Fermi level. Similarly with other LDA calculations, we find incorrectly that CuO is a metal instead of a semiconductor. The calculated partial densities of states both at Cu and at O sites (not shown here) agree well with earlier unpolarized results of Ching *et al.* (1989) and Grioni *et al.* (1989).

It follows immediately from Figs. 3–5, that the pre-peak has a purely quadrupole nature — dipole transitions contribute just to a smooth background in the pre-edge region. Only few $d$ components contribute to the experimental pre-peak significantly, viz., the $d_{xz}$ and $d_{yz}$ components in the cell frame and the $d_{x'y'}$ and, to a lesser degree, the $d_{y'z'}$ component in the local frame. The RS-MS calculation reproduces the pre-peak position and intensity with a reasonable accuracy, however, its $d$ decomposition does not agree with experiment. This is most probably caused by the inadequacy of a non-self consistent muffin-tin potential for this kind of analysis. The band-structure calculation, on the other hand, predicts correctly that $d_{xz}$ and $d_{yz}$ are the dominant components in the cell frame. This remarkable agreement verifies retrospectively also the way of resolving the $d$ components from the experimental spectra, which is quite a complicated procedure (Bocharov *et al.*, 2000).

Our finding that $d_{x'y'}$ represents the most important contribution to the pre-peak in the local frame supports also works of Anisimov *et al.* (1991) and Grioni *et al.* (1989), who found that the lowest unoccupied states in CuO at the Cu site has a $d_{x^2-y^2}$ character. As their coordinate system is rotated by $45°$ with respect to our local frame, their $d_{x^2-y^2}$ orbital actually corresponds to the $d_{x'y'}$ orbital in our notation.

Commonly, a quadrupole character has been attributed to the pre-peak in transition-metal oxides (Sahiner *et al.*, 1995; Saini *et al.*, 1998). A positively established quadrupole nature of the pre-peak in a CuO crystal thus puts earlier tentative assignments, based on analogies with copper oxide, on a solid ground.

When comparing RS-MS calculation of *dipole* components with experiment, we find sometimes a good agreement even in minor details (such as fine structure of the main peaks at 18–25 eV for the $p_{x'}$ and $p_{y'}$ components), however, sometimes there is a significant disagreement between RS-MS theory and experiment. Most notably, RS-MS spectra display a spurious peak around 7 eV, both in the cell and in the local reference frame. The reason for this disagreement could be twofold: Either the inadequacy of the scattering potential, or possibly the breakdown of the one-electron picture itself. While theoretical studies of molecular $CuCl_2$ or $CuCl_4^{-2}$ complexes seem to support the latter explanation (Bair and Goddard, 1980; Yokoyjama *et al.*, 1986), our pseudopotential band-structure calculation removes the worst failures of the RS-MS theory in the cell reference frame, attributing them thus to the deficiency of non-self consistent muffin-tin potential. So we feel there is a strong case to assume that one-electron processes still carry the most dominant contribution to the Cu $K$ edge XANES in CuO.

## 5. Conclusions

We find that the pre-peak in Cu $K$ edge XANES in CuO arises from quadrupole-allowed transitions to the $d_{xz}$ and $d_{yz}$ states in cell reference frame and to the $d_{x'y'}$ states in the local frame. The RS-MS theory based on non-self consistent muffin-tin potential describes the experimental spectra quite well in general, however, some obvious discrepancies arise especially in the shoulder region. Most of these discrepancies can be removed in the cell reference frame by employing a self consistent pseudopotential band structure calculation. The bulk of the XANES structure thus appears to arise from one-electron processes.

## References

Anisimov, V. I., Zaanen, J. & Andersen, O. K. (1991) *Phys. Rev.* B**44**, 943–954.
Bair, R. A. & Goddard III, W. A. (1980). *Phys. Rev.*B **22**, 2767–2776.
Bocharov, S., Kirchner, Th., Dräger, G., Šipr, O. & Šimůnek, A. (2001), to be published in *Phys. Rev.* B.
Brouder, C. (1990). *J. Phys.: Condens. Matter* **2**, 701–738.
Ching, W. Y., Xu, Y.-N. & Wong, K. W. (1989). *Phys. Rev.* B**40**, 7684–7695.
Grioni, M., Czyżyk, M. T., de Groot, F. M. F., Fuggle, J. C. & Watts, B. E. (1989) *Phys. Rev.* B**39**, 4886–4890.
Hahn, J. E., Scott, R. A., Hodgson, K. O., Doniach, S., Desjardins, S. R. & Solomon, E. I. (1982). *Chem. Phys. Lett.* **88**, 595–598.
Norman, D., Garg, K. B. & Durham, P. J. (1985). *Solid State Commun.* **56**, 895–899.
Saini, N. L., Lanzara, A., Bianconi, A. & Oyanagi, H. (1998). *Phys. Rev.* B**58**, 11768–11773.
Sahiner, A., Croft, M., Guha, S., Perez, I., Zhang, Z., Greenblatt, M., Metcalf, P. A., Jahns, H. & Liang, G. (1995). *Phys. Rev.* B**51**, 5879–5886.
Šimůnek, A., Polčík, M. & Wiech, G. (1995). *Phys. Rev.* B**52**, 11865–11871.
Šipr, O. (1992). *J. Phys.: Condens. Matter* **4**, 9389-9400.
Vackář, J., Hytha, M. & Šimůnek, A. (1998). *Phys. Rev.* B**58**, 12712–12720.
Yokoyama, T., Kosugi, N. & Kuroda, H. (1986). *Chem. Phys.* **103**, 101–109.